

On-Line Voltage Security Assessment of the Hellenic Interconnected System

C. D. Vournas, G. A. Manos, J. Kabouris, G. Christoforidis, G. Hasse, T. Van Cutsem

Abstract—This paper describes the on-line Voltage Security Assessment environment developed within the framework of the EU-sponsored OMASES project, as well as its application to the Greek Interconnected Power System. The heart of all computations is a fast time-domain method. Security is analyzed with respect to power transfers in critical corridors or power consumption in load areas. Results take on the form of either pre-contingency secure operation limits, or post-contingency loadability limits, together with various diagnosis tips. Typical results obtained during the test phase of the project are reported.

Index Terms-- Voltage Stability, Voltage Security Assessment, Quasi steady-state simulation, Secure Operation Limits, Loadability limits.

I. INTRODUCTION

Voltage Security Assessment (VSA) is often quoted as one of the much needed applications in control centers [1,2].

This paper describes and reports on the first results of the VSA function developed within the framework of the EU-sponsored OMASES project. The latter aims at developing an on-line platform for dynamic security assessment, training simulation and market simulation [3, 4].

The methods used in OMASES-VSA and their practical implementation are described and a sample of results stemming from its use at the national control center of the Hellenic Transmission System Operator (HTSO) are presented. The reader is kindly invited to refer to the companion paper [5] for a presentation of the OMASES project itself, the main features of the platform, as well as some other results obtained so far.

II. VOLTAGE SECURITY ASSESSMENT METHODS

A. Quasi steady-state simulation : principle and modelling

The heart of all computations performed within OMASES-VSA is Quasi Steady-State (QSS) simulation, a fast time-domain method well suited to the analysis of long-term voltage

stability phenomena [6].

The QSS approximation relies on *time-scale decomposition*. The essence of this method is that faster phenomena are represented by their equilibrium conditions instead of their full dynamics. This greatly reduces the complexity of the resulting model and hence provides the computational efficiency required to meet the constraints of an on-line application. In addition, the amount of additional data required by the QSS model is moderate, so that data collection, validation and maintenance is not a big issue.

This method, which has been previously validated with respect to detailed time simulation [7], offers better accuracy and richer interpretations than simple methods based on load flow equations. For instance, in unstable cases, the area in trouble is automatically pointed out, while complementary diagnosis tools can be run on the unstable system trajectory in order to identify appropriate remedial actions.

Thus, the method offers an interesting compromise between the computational efficiency of static methods and the above advantages of time-domain based approaches.

Under the QSS approximation, the short-term dynamics of a synchronous generator, its governor and its Automatic Voltage Regulator (AVR), are replaced by three nonlinear algebraic equations [6]. The latter account for the generation saturation, the AVR steady-state gain and the speed droop. These nonlinear equations are solved at each time step, together with the network ones.

Each load is typically represented as shown in Fig. 1. Voltage dependent active and reactive powers are assumed at the MV bus behind the HV-MV distribution transformer, in parallel with a shunt compensation capacitor. Load power restoration mainly comes from the Load Tap Changers (LTCs) operating in such transformers.

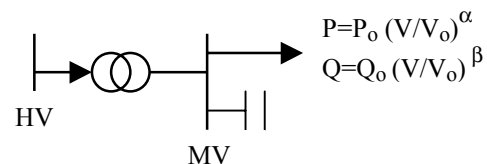


Fig. 1. A typical load model

QSS simulation reproduces the long-term dynamics of LTCs, OverExcitation Limiters (OELs), automatically switched shunt compensation, secondary voltage control (if any), protecting devices, etc. This simulation takes into account the (initial and subsequent) delays in between trans-

Costas D. Vournas and George A. Manos are with the School of Electrical and Computer Eng., National Technical University of Athens, Greece (e-mail: vournas@power.ece.ntua.gr).

John Kabouris and George Christoforidis are with the Hellenic Transmission System Operator, Athens, Greece.

Gaëtan Hasse and Thierry Van Cutsem are with the Dept. of Electrical Engineering and Computer Science (Montefiore Institute) of the University of Liège, Sart Tilman B37, B-4000 Liège, Belgium. T. Van Cutsem is a research director of the Belgian National Fund for Scientific Research (FNRS) (e-mail: t.vancutsem@ulg.ac.be).

former tap changes, the delays before a synchronous machine is switched under constant field current, etc.

B. System stress

The VSA function mainly aims at computing security margins with respect to the risk of voltage instability. These security margins refer to a notion of *system stress*, i.e. a change in load and generation which makes the system weaker by increasing power transfer over relatively long distances and/or by drawing on reactive power reserves. A system stress is characterized by its *direction*, i.e. by the participation of each load active and reactive power to the overall load increase and that of each generator active power production to the overall generation adjustment.

C. Loadability limits

The first type of computations aim at determining *loadability limits*, which indicate how much the system can be stressed before reaching instability. To this purpose, OMASES-VSA does not resort to the standard (repeated or continuation) power flow, but rather simulates the time response of the system to a ramp increase in demand and/or generation. For a load increase, the P_0 and Q_0 coefficients of the load model shown in Fig. 1 are increased linearly with time, taking into account the participation coefficients specified for each load. During this time simulation, voltages at key buses are recorded as a function of the total load in various predefined areas as well as in the whole system, so as to finally produce the familiar PV curves. The rate of change of the powers is chosen small enough to consider that the system evolves through steady states, and large enough to save computing time. The LTCs, OELs, etc. respond with their delays and LTC limits are automatically reflected.

The so computed *pre-contingency loadability limit* provides the operator with an indication of the system ability to stand a sustained load increase, in the absence of disturbance.

Post-contingency Loadability limits (PCLLs) are also computed, for a limited set of dangerous contingencies, whose identification is described in Section II.E. To this purpose, in the same run, the contingency is simulated over a specified time interval, before the ramp increase in demand is applied. Note that for loadability limit calculation corresponding to a load increase, generation adjusts to the actual load increase (which is in general less than the ramp imposed on demand, due to LTC deadbands and limits) according to generator speed droops.

D. Secure Operation Limits

The second type of computations aim at determining *Secure Operation Limits* (SOLs). For a given direction of stress, the SOL corresponds to the most stressed operating point such that the system can withstand any contingency of a specified list.

In the SOL computation:

- the pre-contingency stress assumes full load recovery, and a load flow type of modeling is used, but with accurate generator reactive limits. The load increase is compensated by redispatching generation according to participation factors

- the effect of a contingency is assessed using QSS simulation, initialized at the pre-contingency load flow solution.

Binary search is a simple and robust method to determine the SOL with respect to one contingency. It consists of building an interval $[S_l, S_u]$ of stress values such that S_l corresponds to an acceptable post-contingency evolution, S_u to an unacceptable one, and $S_u - S_l$ is smaller than a specified tolerance Δ . At each step, the interval is divided in two equal parts; if the midpoint is found acceptable (resp. unacceptable) it is taken as the new lower (resp. upper) bound. The procedure is illustrated in Fig. 2, where the dashed arrows show the sequence of tested stress levels.

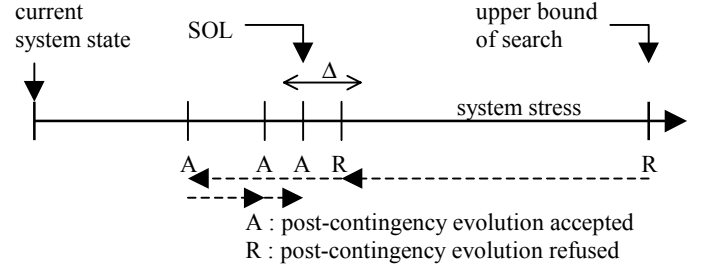


Fig. 2. Binary search of a single SOL

The search is automatically performed on the interval $[0, \min(S_{max}, f \cdot S_N)]$ whose lower bound corresponds to the present system state, and where S_{max} is a maximum stress of interest, S_N the maximum stress that can be reached in the absence of contingency and f is typically equal to 0.9.

To deal with several contingencies, it is advantageous to perform a *Simultaneous Binary Search* (SBS). At a given step of this search, the various contingencies stemming from the previous step are simulated. If at least one of them is unacceptable, the acceptable ones are discarded (since their limits are higher than the current stress) and the search proceeds with the unacceptable ones only. For the most severe contingency(ies), the SOL is computed with the Δ accuracy, while for the others, a lower bound on the SOL is obtained. The smaller the SOL, the more accurate this lower bound.

A simple example with 4 contingencies is shown in Fig. 3. The most severe contingency is the first one, and its SOL is thus the overall SOL. The SOL of contingency no. 3 is in the interval $[S_l, S_0]$ while that of contingency no. 2 in $[S_3, S_l]$.

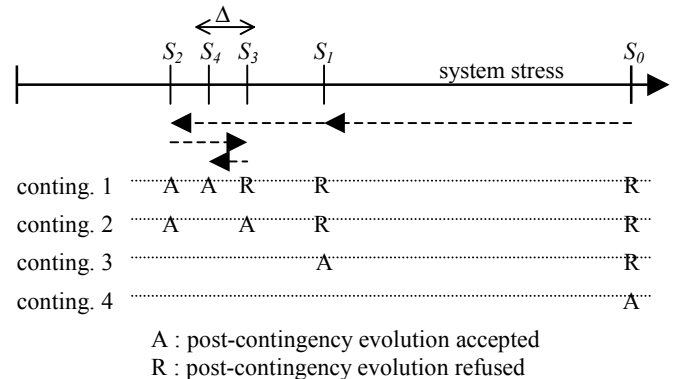


Fig. 3. Simultaneous binary search of the most severe SOL

Of course, one may also specify a level of stress below which *all* limits are sought (at an extra computational cost) with the Δ accuracy.

E. Contingency filtering

Contingency filtering is an important step of any on-line security assessment. A form of filtering takes place at the first step of the SBS, i.e. at maximum stress, when discarding the contingencies which yield an acceptable system response. However, in spite of the QSS simulation speed, it may take too long to simulate the system response to each contingency of a long list. An additional *pre-filtering* may be needed before the SBS is launched. In a majority of systems, post-contingency load flows can be advantageously used to this purpose.

Load flow equations with constant power loads and enforcement of generator reactive limits correspond to the long-term equilibrium that prevails after load voltage restoration by LTCs and machine excitation limitation by OELs. Insofar as voltage instability results from the loss of such an equilibrium, the corresponding load flow equations no longer have a solution and the Newton-Raphson algorithm diverges. On the other hand, divergence may result from purely numerical problems and some dynamic controls that help stability cannot be accounted for in the static load flow calculation. Conversely, some system dynamics may be responsible for an instability not detected by the load flow.

Keeping in mind the above conflicting aspects, the filtering consists of : (i) performing QSS simulation on a subset of contingencies labelled *potentially harmful*; (ii) identifying the latter as the contingencies that cause the load flow to diverge or some voltages to drop by more than a threshold ΔV .

The value of ΔV must be taken large enough to filter out as many harmless contingencies as possible, but not too large to avoid missing a contingency with low SOL.

To make the filtering as reliable as possible, the post-contingency load flow data must closely match the QSS model. To this purpose, the reactive power limits of the generators are updated with their active power and terminal voltages, while active power imbalances are distributed over them according to frequency control.

Note finally that the PCLLs and PV curves described in Section II.C are computed for the subset of contingencies found with the lowest margins at the end of the SOL determination (which is thus performed first).

F. Diagnosis tools in expert mode

The outputs automatically produced by the SOL and PCLL computations will be presented in Section V. In addition to these, OMASES-VSA has an “expert mode” giving access to complementary diagnoses.

The latter are mainly based on sensitivity and/or eigenanalysis and provide the following type of information.

In case of long-term voltage instability, an analysis of the long-term Jacobian allows to rank the bus active and reactive power injections by decreasing order of their effectiveness in counteracting the instability, thereby pointing out where gen-

eration should be rescheduled or committed, or load shed.

When a singularity of the QSS time evolution has been met, corresponding to the loss of a short-term equilibrium [6], the short-term Jacobian is analyzed to find which generators are mostly responsible for the loss of synchronism.

III. IMPLEMENTATION WITHIN THE OMASES PLATFORM

The architecture of OMASES-VSA is shown in Fig. 4.

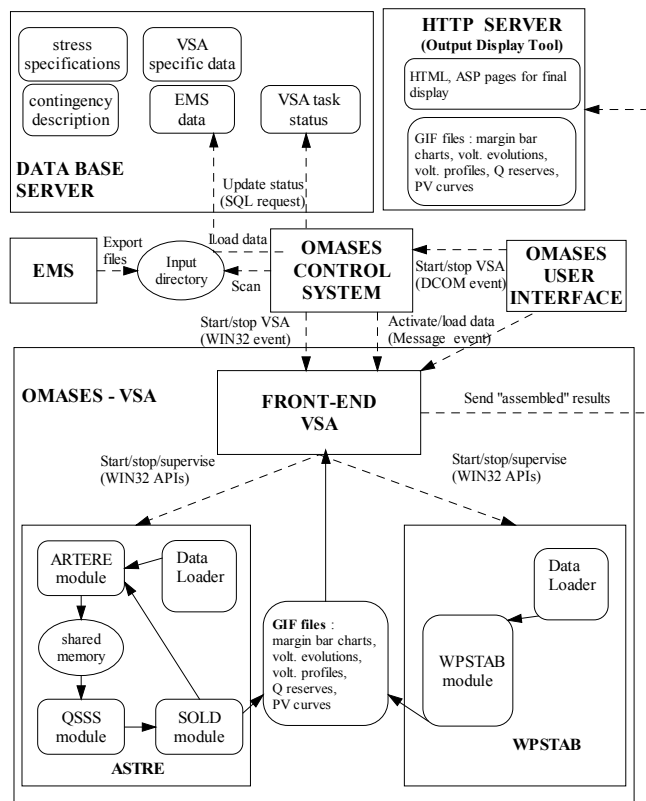


Fig. 4. Architecture of the VSA application within the OMASES platform

A. VSA software

OMASES-VSA integrates two VSA software packages developed prior to the OMASES project.

The SOL computation and the contingency filtering rely on the ASTRE software developed at the University of Liège and used by several power companies [6,7,8]. ASTRE itself is made up of a load flow program (ARTERE, used for stressing the system and filtering contingencies) and a QSS simulator (QSSS, used for simulating contingencies) both “conducted” by the SOLD module implementing the binary searches. The former two executables communicate through a shared memory for the data and through files for the outputs.

The computation of PCLLs and the production of PV-curves rely on the WPSTAB software previously developed at the National Technical University of Athens [9].

Within the context of OMASES, data loaders have been devised whose rôle is to connect (through SQL requests) to the relational data base server hosting the Energy Management System (EMS) data, the VSA-specific data, the stress speci-

cation, the contingency description, and the output curves description. The data loaders produce the ASCII files needed by ASTRE and WPSTAB.

The outputs of ASTRE and WPSTAB consists of GIF figures showing plots and ASCII files with numerical results.

B. Other VSA-related modules

Among the other modules sketched in Fig. 4, let us quote:

- the OMASES Control System, aimed at: queuing and dispatching OMASES messages to the VSA task, detecting the presence of new EMS files, loading them into the database through a loader script, activating, synchronising and supervising the VSA task automatically, updating its status into the database;
- the Omases User Interface, aimed at: starting and stopping the VSA task, activating it manually, making the VSA task status visible to the OMASES user.

Last but not least, a “front-end” program has been developed in order to: prepare, manage and remove dynamically the working environment of a new VSA session, communicate (through messages) with the remaining of the OMASES environment, launch the data loaders, call sequentially and supervise the ASTRE and WPSTAB programs, collect the GIF figures produced by the latter and assemble them into HTML pages, together with ASP scripts, for user-friendly WEB-based display by the HTTP server (the latter being used for both controlling the platform and displaying results).

IV. IMPLEMENTATION AT THE HTSO CONTROL CENTER

The VSA application has been installed and is currently in operation within the OMASES platform at the National Control Center of HTSO. OMASES-VSA relies on a WINDOWS server, hosting the relational database system, running the VSA computations, and connected through a Local Area Network (LAN) under the TCP/IP protocol.

The above server is separate from the mainframe computer, which runs under the VMS operating system and hosts the “closed” EMS platform and hierarchical databases. The communication between the EMS and OMASES computers is accomplished with text files loaded by the EMS host onto the OMASES server.

Two modes of operation of OMASES-VSA are most often used: the real-time and study modes, whereas in the expert mode the experienced users can have access to more analysis tools, such as those outlined in Section II.F.

A. Real-time mode

In this mode of operation, OMASES-VSA is coupled to the real-time EMS system. Therefore, although the period of execution of OMASES-VSA is in the range of every 10-30 minutes, this mode is referred to as the real-time mode.

In this configuration, the EMS feeds OMASES-VSA with network state estimator solutions. The execution of the VSA functions is periodic and triggered automatically by the data transfer from the EMS. More precisely, an EMS process periodically creates 14 text files containing the latest network so-

lution computed by the state estimator. Each file is a description of a class of EMS components (e.g. substations, nodes, buses, lines, transformers, generators, loads, etc.) and corresponds to a table of the VSA relational database. These files are sent by the same EMS process to a predefined real-time entry directory of the VSA server, which triggers the VSA computation cycle.

If the EMS cycle (period of state estimator) is shorter than the VSA cycle, the VSA process will not be interrupted; new EMS data set will be loaded as soon as the previous VSA cycle finishes. After the fine tuning performed during the experimentation phase of the OMASES project, the whole VSA cycle takes 3 to 4 minutes on the average (on a Pentium IV PC)

The VSA results are stored in the database when the analysis is completed and the WEB-based user interface is used to display results on PCs connected to the LAN.

B. Study mode

In this mode, the execution of OMASES-VSA is launched manually by the user. The data used may be either the real-time data or saved snapshots retrieved from the historical database by the user. A network solution stemming from the EMS state estimator or from a power flow program (saved cases) can thus be retrieved from the database dedicated to study mode, and used to initialize a VSA study.

V. VSA ANALYSIS OF THE HTSO SYSTEM

A. VSA of the Greek interconnected system

The Greek transmission system serves the mainland of Greece and some interconnected islands. It consists of 400 and 150-kV networks. The system is interconnected to the Balkan countries (Albania, Bulgaria, and FYROM) via three 400-kV tie lines, and to Italy via an asynchronous 400-kV AC-DC-AC link put in operation in 2002.

The main production center is in Northern Greece in the vicinity of a lignite rich area. The thermal power plants of this region produce about 70% of the total electricity of the Greek mainland. Significant hydro production exists in the North and Northwest of the country, while another lignite production is available in the Southern peninsula of Peloponnese.

The main consumption is in the metropolitan area of Athens. This leads to significant power transfers from North to South. Several critical operating conditions are associated with this geographical imbalance of generation and load especially in cases of reduced availability of the local generation in the Athens area and/or Peloponnese. These critical conditions are mainly linked to voltage problems following contingencies.

In this section, typical outputs of OMASES-VSA are presented for two snapshots of interest: a winter and a summer case, respectively. The winter case was obtained in real-time mode and corresponds to a relatively high load of the Greek system that occurred on Feb.11, 2003. The summer case corresponds to the maximum system load for 2002, which occurred on July 16. It was produced in study mode from a saved EMS

case (at that time, OMASES-VSA was not yet installed at HTSO).

The stress considered for the VSA analysis is the default one, corresponding to a national load increase covered by the local generation reserve. Other system stresses, such as a load increase in the southern part of the system, a generation decrease in certain areas, or an increase of power flow from or to the external interconnections can be selected by the OMASES-VSA user, but are not considered in this paper.

The set of all N-1 contingencies and some probable N-2 ones, for a total of 433 contingencies, was considered.

B. Summer 2002 case

Starting from the summer 2002 snapshot as a base case and applying a national load increase, the contingencies resulting in the most constraining SOLs are listed in Table I, together with the corresponding margins. The latter have been computed with a tolerance $\Delta = 10$ MW.

TABLE I. SECURE OPERATION MARGINS (SUMMER CASE)

no.	contingency name	margin (MW)
329	LINE_CON TMOYΔAN-MOYΔ.1	0
296	LINE_CON MOYPT-MESOΓ.1	0
228	LINE_CON ΚΘΕΣ-ΣΧΟΛΑΡ.1	0
312	LINE_CON ΜΕΣΟΓΓ-ΚΕΡΚ2.1	0
109	LINE_CON ΑΡΓ2-ΑΡΓ1.1	73
347	LINE_CON ΣΧΗΜ-ΘΗΒΑ.1	94
69	GEN_CON Κ_ΛΑΥΠΙΟ.GFIC.UN	146
58	GEN_CON ΛΑΥΠΙΟ.GFIC.GEN2.UN	167
90	LINE_CON ΑΓΡΑΣ-ΣΚΥΔΡΑ.1	292
388	LINE_CON ΦΙΛΙΠ-ΑΜΦΙΠΟ.1	324
22	GEN_CON ΑΓ.ΓΕΩΡΓ.GEN9.UN	470
	all other contingencies	> 668

The first four contingencies have a zero margin, meaning that the occurrence of any of these at the specific time the snapshot was taken would result in unacceptable post-contingency conditions. As it turned out, however, these contingencies, as well as the next two of Table I, result in very local problems, already known to HTSO operators. The nature of these problems is the breaking-up of a loop resulting in very long radial path to a relatively large load and hence in an excessive voltage drop.

The extent of the problems caused to the system by an unacceptable contingency is easily assessed from the “voltage profiles” automatically produced by the SOL computation. A voltage profile is obtained by taking a snapshot of the collapsing system at the marginally refused stress, and showing the number of buses with voltages below a certain level. The affected area is identified from the names of typical buses. For instance, Fig. 5 shows the voltage profile corresponding to contingency No 329, the first one in Table I. As can be seen, very few buses are involved. This situation is known to HTSO and network reinforcements in all areas exhibiting this type of local voltage problems are under way.

Similarly, Fig. 6 shows the voltage profile for the first system-wide dangerous contingency, namely the loss of the com-

bined cycle plant in K_Lavrio (no. 69, see Table I). As seen in this figure, the disturbance is widely spread, even though the focal point is in the Central Greece region just to the north of Athens metropolitan region. This picture is typical of a wide instability mode.

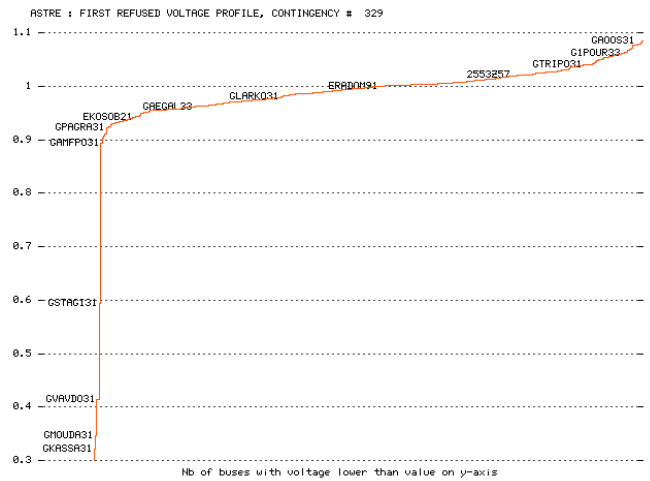


Fig. 5. Voltage profile for a contingency with very local impact

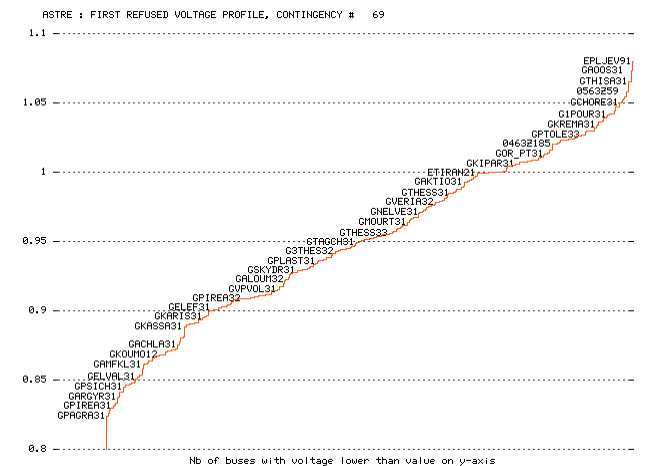


Fig. 6. Voltage profile for a contingency with system-wide impact

Another output readily available for interpreting results is the post-contingency time evolution of the lowest transmission voltage at the marginally accepted and refused stresses, respectively. In the case of the Greek system, contingencies are simulated over a time interval of 900 s, unless a singularity is met before, corresponding to loss of synchronism. If not, the final voltages are compared to a lower acceptable value, typical of a partial voltage collapse (in this case 0.7 pu) to decide whether the system evolution is acceptable or not.

Figure 7 shows the voltage evolution for contingency no. 347 (see Table I). The contingency is applied at $t = 10$ s. As can be seen, the marginally refused case does not correspond to a voltage instability but merely to final voltages that are a little below the 0.7 pu threshold. Hence, for this contingency, the SOL should not be interpreted as a stability limit.

A quite different situation is shown in Fig. 8, relative to contingency no. 69. Here, the marginally unstable simulation

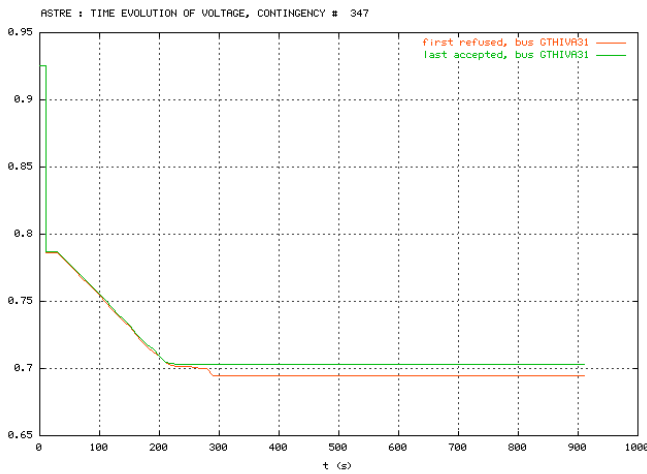


Fig. 7. Post-contingency voltage evolutions: low but stable voltages

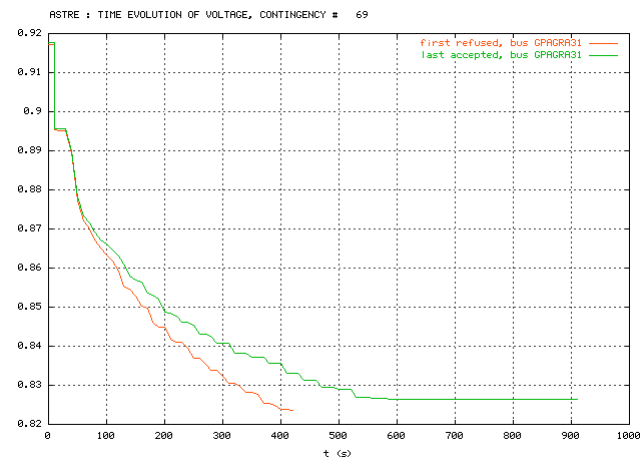


Fig. 8. Post-contingency voltage evolutions near a stability limit

ends up in a loss of synchronism at $t = 420$ s.

One of the main causes of voltage instability is the reactive limitation of generators imposed mainly by OELs. An additional output of the SOL computation shows the degree of involvement of the various generators in the instability mechanism. One such plot is shown in Fig. 9. The involved generators are those that respond significantly to the disturbance. For each of them:

- the largest bar shows the *physical capability*, i.e. the reactive power production when the field current is at its limit;
- the middle bar shows the *effective capability*, defined as the post-contingency production when the system has been previously stressed at the SOL. The difference between the physical and effective capabilities is the fraction of the reactive reserve that cannot be used to face the contingency;
- the smallest bar shows the post-contingency production in the base case (at no stress). If the latter was equal to the effective capability, the system would have no security margin with respect to the contingency of concern.

The next four figures show (national or regional) PV curves obtained during loadability limit determination, as explained in Section II.C.

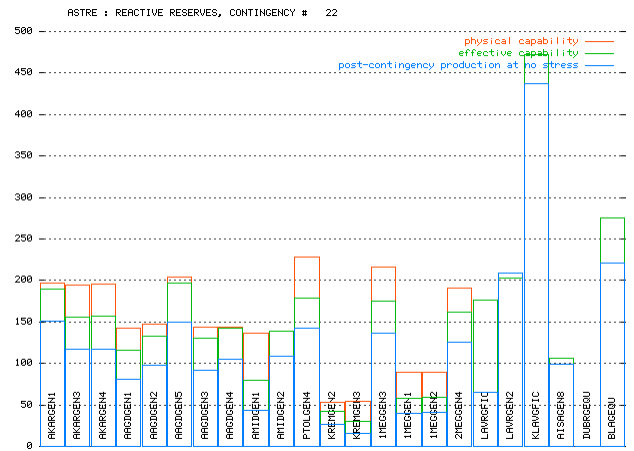


Fig. 9. Overview of generator reactive powers

Figure 10 corresponds to the total system load and has been obtained by simply increasing load demand in the base case. This result tells the operator how far the system can go even without contingencies. As seen from the figure, the load can increase by more than 500 MW in the absence of any contingency.

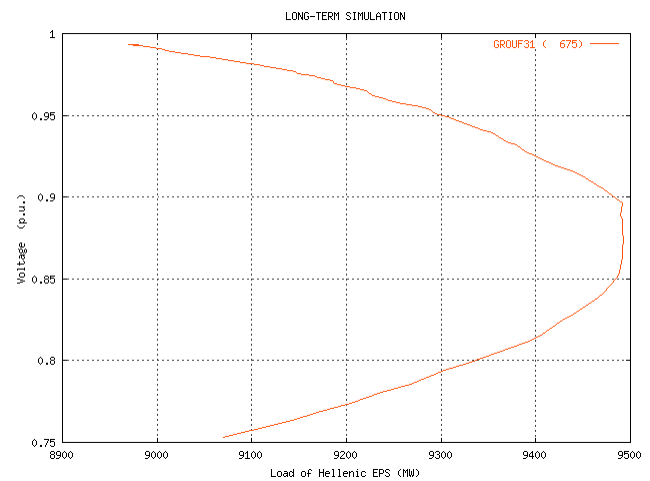


Fig. 10. Characteristic transmission bus voltage vs system load power

PCLLs are obtained by stressing the system after contingencies. For instance, Figs. 11-13 correspond to the system evolution under the effect of contingency no. 69 (first critical, loss of K_Lavrio), followed by a ramp increase in demand.

As can be seen in Fig. 11, this is a very severe contingency and the total load is barely able to restore its precontingency consumption even after the demand ramp. This is due to the exhaustion of the regulating range of the LTCs in the most affected area, as well as in some substations of the Athens region. At these places the power received by consumers is reduced due to low distribution voltages. Note that due to the non-restoration of load, the PCLL implied in Fig. 11 should not be compared to the SOL margin of Table I, for which the stress is applied prior to the contingency assuming full restoration of load power.

The PV curve of Fig. 12, relative to the Athens region, shows that the latter is able to first restore, then increase its

load despite the low voltages at certain transmission buses. The PV curve of the mostly affected area of Central Greece is shown in Fig. 13. Clearly, in this case, the load power is severely reduced after the contingency and the increased demand increase cannot lead to increased consumption. Customer service in this area will greatly suffer if such a contingency occurs.

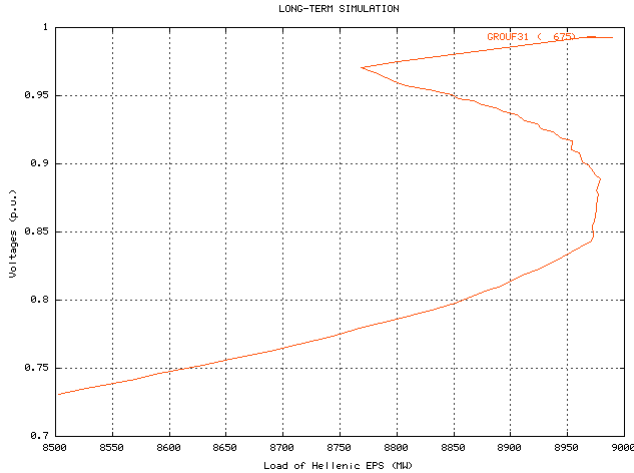


Fig. 11. PV curve after contingency no. 69; national load power

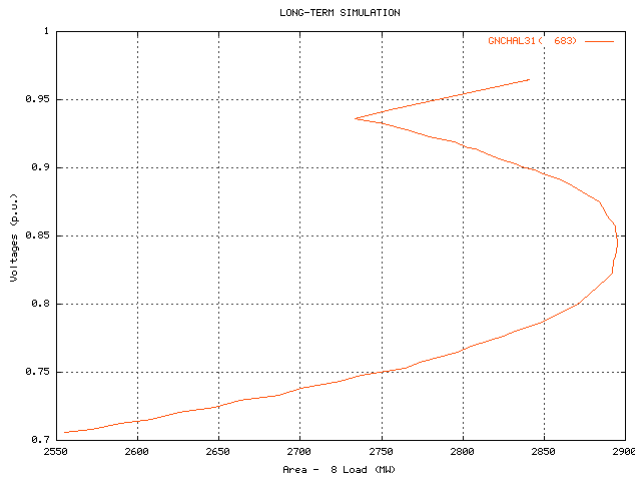


Fig. 12. PV curve after contingency no. 69; Athens region load power

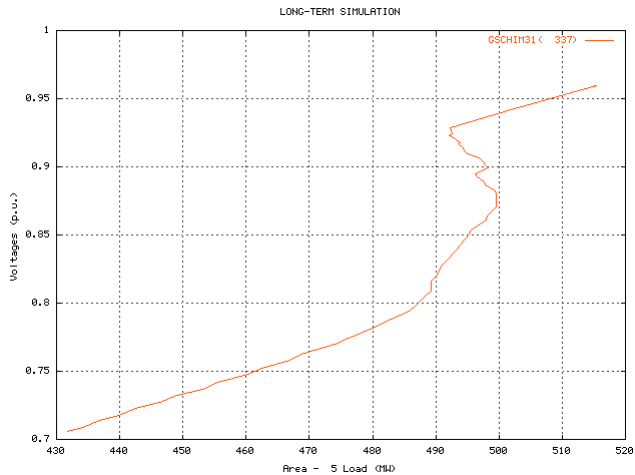


Fig. 13. PV curve after contingency no. 69; Central Greece load power

C. Winter 2003 case

This interesting case was encountered during the on-line application of OMASES-VSA. On February 11, 2003 one natural gas power station (AHSAG) in the Athens area was not in operation, which left the region with little reactive support. Although the total load was considerably lighter than that of the summer peak, the first contingency with system-wide effects has a very small SOL.

As seen in Table II, five contingencies appear with zero margin. Three of these are the same as in Table I. Of the two new contingencies, no. 254 is similar to 296 and 312 and is related to the breaking of the loop feeding via two cables the island of Corfu. Contingency 299 involves the line connecting Greece to Albania. As seen in Fig. 14, this contingency only affects the external equivalent of the system (bus names starting with E).

TABLE II. SECURE OPERATION MARGINS (WINTER CASE)

contingency		margin (MW)
no.	name	
254	LINE_CON KEPK2-KEPK1.1	0
312	LINE_CON ΜΕΣΟΓΓ-ΚΕΡΚ2.1	0
299	LINE_CON KARD-ELBA400.1	0
296	LINE_CON ΜΟΥΡΤ-ΜΕΣΟΓ.1	0
228	LINE_CON ΚΘΕΣ-ΣΧΟΛΑΡ.1	0
61	LINE_CON Κ_ΛΑΥΠΙΟ.GFIC.UN	40
51	GEN_CON_ΛΑΥΠΙΟ.GFIC.GEN2.UN	79
all other contingencies		> 316

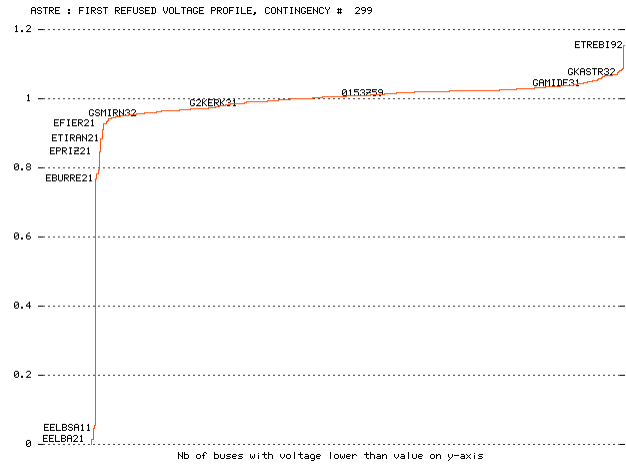


Fig. 14. Voltage profile for contingency no. 299

Contingency no. 61, with a system-wide impact, is again the loss of the combined cycle plant in K_Lavrio. The margin of this contingency is only 40 MW ! However, as this snapshot was taken at the daily peak and the load was already ramping down it was not deemed necessary to start the units in AHSAG.

As in the summer case, the most affected area is the Central Greece to the north of Athens, as confirmed by the corresponding PV curve of Fig. 15. The load in this area cannot increase at all after the contingency, due to the LTCs hitting their limits. The outcome of the long-term voltage instability is a loss of synchronism. As seen in Fig. 16, the latter takes place

VI. CONCLUSION

This paper has described the advanced on-line VSA application developed within the context of the EU-sponsored project OMASES. This tool has been implemented, tested and tuned at the Greek national control center of HTSO.

This paper has also reported on preliminary results from this on-site experimentation.

The use of this on-line VSA tool during the testing period has demonstrated some, already known, local voltage problems. Beyond this, the main benefit expected by HTSO from such a tool is the possibility to better know the system limits and operate closer to them.

More specifically, since the local generation in the Athens area is significantly expensive, it is usually driven out of the market by the everyday bidding procedure. In case of reduced security margins, this generation is put in operation (must-run units) in order to alleviate transmission constraints and increase security. Since the operation of expensive units increases the uplifts in the electricity market, it is a major concern for HTSO to avoid such practices and try to operate the system closer to its limits.

On-line VSA is the most crucial tool to achieve this task. It is expected to facilitate the every-day operation by allowing more accurate estimations of the secure operating limits. The use of traditional static security analysis leads sometimes to either start expensive generation in the area of Athens or shed loads while it is not necessary. Such a situation has been avoided during the winter peak of this year.

Finally, the use of the on-line VSA tool will contribute significantly to the training of the operators, will allow a better understanding of voltage instability phenomena and will make it easier to evaluate, using the expert mode, the benefit of countermeasures against credible disturbances.

VII. REFERENCES

- [1] B.Gao, G.K. Morison, P. Kundur, "Towards the development of a systematic approach for voltage stability assessment of large-scale power systems", IEEE Trans. on Power Systems, Vol. 11, pp. 1314-1324, 1996
- [2] "Techniques for power system stability limit search", IEEE special publication IEEE TP-138-0, Jan. 2000
- [3] A. Bihain, G. Burt, F. Casamata, T. Koronides, R. Lopez, S. Massucco, D. Ruiz-Vega, C. Vournas, "Advance Perspectives and Implementation of Dynamic Security Assessment in the Open Market Environment", paper 39-101, CIGRE 2002.
- [4] C. D. Vournas, G. A. Manos, G. Hasse, T. Van Cutsem, "On-Line Voltage Security Assessment within the OMASES Project", Proc. of the MedPower 2002 Conference, Athens, Nov. 4-6, 2002
- [5] A. Bihain, D. Cirio, M. Fiorina, R. Lopez, D. Lucarella, S. Massucco, D. Ruiz Vega, C. Vournas, T. Van Cutsem, L. Wehenkel, "OMASES: A Dynamic Security Assessment Tool for the New Market Environment", paper to be presented at the IEEE Bologna Power Tech conf., June 2003
- [6] T. Van Cutsem, C. Vournas, Voltage Stability of Electric Power Systems, Kluwer Academic Publishers, Boston, 1998.
- [7] T. Van Cutsem, R. Mailhot, "Validation of a fast voltage stability analysis method on the Hydro-Québec system", IEEE Trans. on Power Systems, Vol. 12, pp. 282-292, 1997
- [8] T. Van Cutsem, F. Capitanescu, C. Moors, D. Lefebvre, and V. Sermanon, "An advanced tool for preventive voltage security assessment", Proc. VIIth SEPOPE conference, Curitiba (Brazil), 2000, paper IP-035
- [9] C. Vournas, Scientific Co-ordinator, "Software Development for Voltage Stability Analysis", Project 96 SYN 95, NTUA, Greece

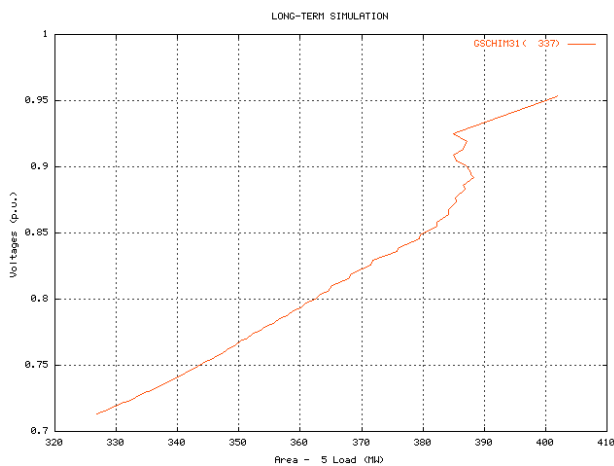


Fig. 15. PV curve after contingency no. 61; Central Greece load power

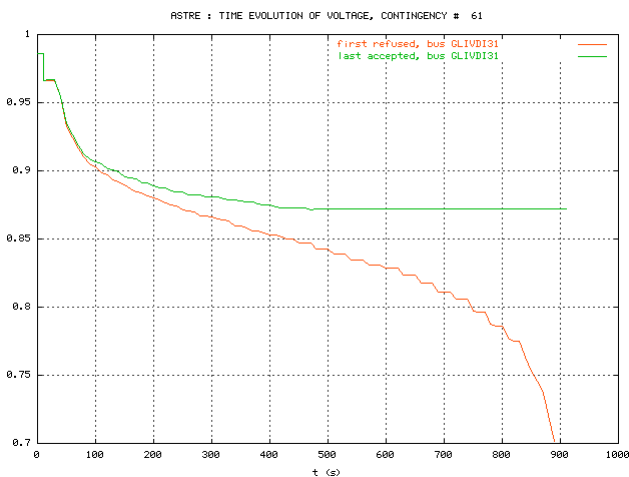


Fig. 16. Post-contingency voltage evolution

when the unstable voltage evolution ends up with an abrupt drop. This evolution is very different from those of Figs. 7 and 8.

The diagnosis provided by OMASES-VSA in expert mode indicates that the loss of synchronism occurs at the Aliveri power station. This is confirmed by Fig. 17, showing the rotor angle curves of the two generators of this station as well as that of a generator in Northern Greece, for comparison purposes.

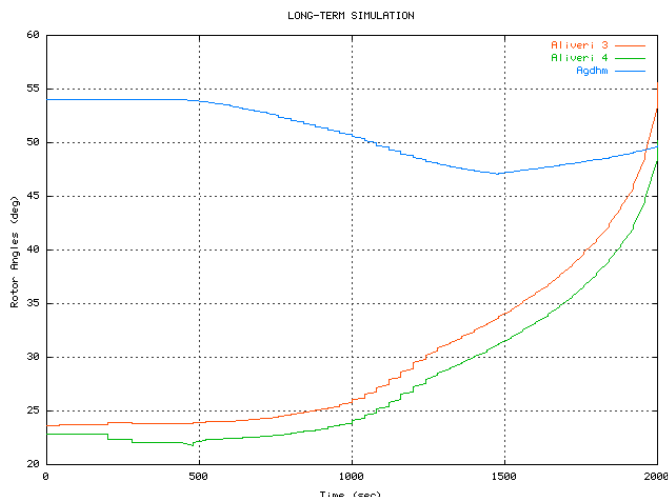


Fig. 17. Rotor angles of Aliveri and AgDhm generators (contingency no. 61)